2686–2693 *Nucleic Acids Research, 1998, Vol. 26, No. 11*

Characterisation of *Bacillus stearothermophilus* PcrA helicase: evidence against an active rolling mechanism

L. E. Bird, J. A. Brannigan[1], H. S. Subramanya and D. B. Wigley*

Sir William Dunn School of Pathology, University of Oxford, South Parks Road, Oxford OX1 3RE, UK and
[1]Department of Chemistry, University of York, Heslington, York Y01 5DD, UK

Received February 9, 1998; Revised and Accepted April 17, 1998

ABSTRACT

PcrA from *Bacillus stearothermophilus* is a DNA helicase for which, despite the availability of a crystal structure, there is very little biochemical information. We show that the enzyme has a broad nucleotide specificity, even being able to hydrolyse ethenonucleotides, and is able to couple the hydrolysis to unwinding of DNA substrates. In common with the *Escherichia coli* helicases Rep and UvrD, PcrA is a 3′–5′ helicase but at high protein concentrations it can also displace a substrate with a 5′ tail. However, in contrast to Rep and UvrD, we do not see any evidence for dimerisation of the protein even in the presence of DNA. The enzyme shows a specificity for the DNA substrate in gel mobility assays, with the preferred substrate being one with both single and double stranded regions of DNA. We propose that these data, together with existing structural evidence, support an inchworm rather than a rolling model for 3′–5′ helicase activity.

INTRODUCTION

Helicases utilise the energy of nucleotide hydrolysis to unwind nucleic acid duplexes. They are involved in many aspects of DNA and RNA metabolism, such as replication, recombination, repair and transcription (1–3). A large number of putative helicases have been identified through sequence homology in both prokaryotes and eukaryotes (4). There are five families based on sequence composition. In addition, where helicase activity has been demonstrated, they can be classified further according to substrate specificity. 5′–3′ helicases require a covalently attached flanking 5′ single-stranded (ss) region of nucleic acid, whereas 3′–5′ helicases require a 3′ ss flanking region. However, although some proteins, such as DnaB and bacteriophage T7 gene 4 proteins, unwind DNA with a 5′–3′ directionality, they show preference for substrates that have both 5′ and 3′ ssDNA at the unwinding junction (5,6). Moreover, at high protein to duplex ratios, the *Escherichia coli* 3′–5′ DNA helicases, helicase II (UvrD) and Rep, will unwind blunt duplexes (7).

The PcrA helicase from *Bacillus stearothermophilus* is a homologue of the PcrA protein from *Staphylococcus aureus*. It also shows considerable homology to both *E.coli* UvrD and Rep (J.Brannigan *et al.*, unpublished data). PcrA in *S.aureus* is essential for cell viability (8) and has been suggested to play a role in rolling circle replication of the plasmid pT181 similar to that proposed for *E.coli* Rep in replication of a number of bacteriophages including ϕX174 (8–10). PcrA from *S.aureus* was inferred to be a helicase through sequence homology (8). More recently, *B.stearothermophilus* PcrA has been cloned and overexpressed (J.Brannigan *et al.*, unpublished data). We have also determined the structure of PcrA by X-ray crystallography (11). However, compared with *E.coli* Rep and UvrD helicases, the biochemical properties of PcrA helicase are characterised poorly.

In this paper we describe the preliminary biochemical characterisation and crystallisation of *B.stearothermophilus* PcrA. PcrA was shown to be a 3′–5′ helicase with a broad specificity for nucleotides. In contrast to both Rep and UvrD, the protein appears to be monomeric under all the conditions tested. In addition we have obtained two crystal forms of PcrA, both of which contain monomeric protein. One crystal form was used previously to determine the structure of PcrA (11). The alternative crystal form should allow the structural determination of the C-terminal domain that was disordered in the original structure.

MATERIALS AND METHODS

Materials, proteins, DNA and nucleotides

Single stranded M13mp18 was purified as described previously (12). Oligonucleotides were synthesised using an Applied Biosystems 381A DNA synthesiser. $p(dT)_4$ and $p(dT)_{10}$ were purchased from Sigma. Nucleotides, nucleotide analogues and dimethylsuberimidate.HCl (DMSI) were purchased from Sigma. Radiolabelled nucleotides were purchased from Amersham.

Purification of PcrA

The following procedure is for 2 l of induced cells. Sonication was carried out on ice, centrifugation at 4°C, and all other steps were at room temperature. One litre cultures of Luria-broth containing 100 μg/ml ampicillin and 34 μg/ml chloramphenicol were each inoculated with a 5 ml culture of B834(DE3) pLysS pBSHII (the overexpressing cell line). The cultures were grown with shaking at 37°C until the A_{600} reached 0.5–0.6. The cultures were induced by the addition of 1 mM IPTG. Growth was continued for 3 h before the cells were harvested by centrifugation

*To whom correspondence should be addressed. Tel: +44 1865 285479; Fax: +44 1865 275515; Email: wigley@eric.path.ox.ac.uk

at 5000 *g*. The cell pellets were resuspended in 20 ml of buffer A [50 mM Tris pH 7.5, 2 mM EDTA, 1 mM dithiothreitol (DTT)], + 200 mM NaCl and 10% sucrose, and frozen at –80°C until required. The cells were thawed and lysed by sonication in the presence of 100 µM phenylmethylsulphonyl fluoride. The supernatant was clarified by centrifugation at 20 000 *g* and then precipitated by the addition of 0.7 vol of saturated ammonium sulphate. The precipitate was harvested by centrifugation at 20 000 *g*. The pellet was resuspended in buffer A in a volume such that the conductivity of the solution was equal to the conductivity of buffer A + 300 mM NaCl. This was applied to a 20 ml heparin–Sepharose column (Pharmacia) pre-equilibrated with buffer A + 100 mM NaCl. Since the protein is less soluble at low salt concentrations, the sample was diluted to a conductivity equal to buffer A + 100 mM NaCl immediately prior to loading onto the column, by using a gradient mixer valve. The column was washed with 2 column volumes of buffer A + 100 mM NaCl and the protein eluted with a 160 ml gradient of 100–600 mM NaCl in buffer A. The peak fractions were pooled and applied to a 50 ml Blue-sepharose column pre-equilibrated with buffer A + 100 mM NaCl. The sample was again diluted while loading to a conductivity equal to buffer A + 100 mM NaCl. The column was washed with 2 column volumes of buffer A + 100 mM NaCl and the protein was eluted with a 250 ml gradient of 100–700 mM NaCl in buffer A. The peak fractions were pooled and precipitated by the addition of an equal volume of saturated ammonium sulphate. The precipitate was harvested by centrifugation at 20 000 *g* and was resuspended in 5 ml of buffer A + 200 mM NaCl. The trace protein contaminants were removed by gel filtration using a Superdex S200 column (Pharmacia). The column was equilibrated with buffer A + 200 mM NaCl. Prior to storage of the protein at –80°C, glycerol was added to the protein pool to a final concentration of 10% v/v. The purity of the sample was monitored by SDS–PAGE on a 10% gel (Fig. 1).

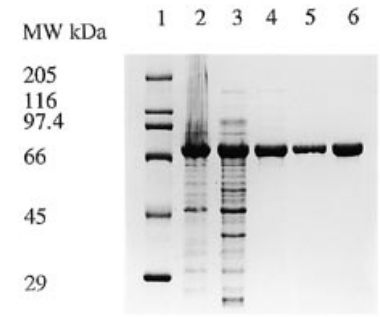

Figure 1. Purification of PcrA. Lane 1, Dalton VII low molecular weight markers; lane 2, clarified sonicated supernatant; lane 3, ammonium sulphate precipated crude extract resuspended in buffer A + 300 mM NaCl; lane4, pooled protein from heparin–Sepharose column; lane 5, pooled protein from Blue-sepharose column; lane 6, pooled protein from gel-filtration column.

Crystallisation of PcrA

The protein was concentrated to 10 mg/ml using Centricon concentrators (Amicon) and exchanged into 50 mM Tris pH 7.5, 300 mM NaCl during this process. Crystals of the PcrA without ligands were obtained by vapour diffusion at 20°C in hanging drops (4 µl) over a 1 ml well solution of 100 mM MES pH 6.4, 1.0 M sodium acetate. An alternative crystal form of PcrA was obtained in the presence of ssDNA and MgADP by vapour diffusion at 20°C in hanging drops (4 µl) over a 1 ml well solution of 100 mM Tris pH 9.0 and polyethylene glycol of molecular weight 8000 at a concentration of 2% (w/v). The protein was buffer exchanged as described previously and was diluted to 7 mg/ml with 50 mM Tris pH 7.5, 300 mM NaCl. ADP to 3 mM, oligo-dT (of defined lengths) to 84 µM and $MgCl_2$ to 10 mM were also added at this point.

X-ray data collection

X-ray data for the apo-crystals were collected using synchrotron radiation (Daresbury, UK) and a MAR image plate detector. Data for the crystals grown in the presence of MgADP and DNA were collected using a Rigaku rotating anode X-ray generator and a MAR image plate detector. The data were processed using DENZO and scaled together with SCALEPACK (13).

DNA helicase assay

The assay conditions were essentially as described previously except that a range of nucleotides was employed at a concentration of 1 mM (14). A 68mer oligonucleotide, with 22 bases homologous to M13mp18 and 5′ and 3′ tails of ssDNA, annealed to ss M13mp18 DNA was used as a substrate (15).

DNA helicase directionality assay

A 12mer oligonucleotide (complementary to nt 6248–6259 of M13mp18 which includes the *Bam*HI site of the polylinker) was annealed to ss M13mp18 DNA, which was then linearised by cutting with *Bam*HI (Gibco-BRL). The linearisation of the DNA was checked by agarose gel electrophoresis. The linearised ssDNA was separated from the digested oligonucleotide by heating the reaction mix to 95°C and passing it through a S400 microspin column (Pharmacia). 22mer oligonucleotides complementary to bases 6230–6251 or 6252–6273 were 5′-end labelled using T4 polynucleotide kinase (New England Biolabs), the unreacted [γ-^{32}P]ATP was removed by centrifugation through a S200 microspin column. The oligonucleotides were annealed to the linearised M13mp18 DNA to give substrates flanked with either 5′ or 3′ ssDNA, respectively.

The reactions (10 µl) contained 20 mM Tris pH 7.5, 100 mM sodium chloride, 3 mM $MgCl_2$, 5 mM DTT, 10% glycerol, substrate, enzyme and 3.0 mM ATP. Each reaction was incubated at 37°C and stopped using 0.2 vol of 2% SDS, 200 mM EDTA and 50% glycerol. The mixture was electrophoresed through a non-denaturing 6% polyacrylamide gel containing TBE. After electrophoresis the gel was fixed, dried under vacuum and auto-radiographed overnight at –80°C with Fuji RX X-ray film.

Nucleotide hydrolysis assay

NTP hydrolysis was monitored by following the production of inorganic phosphate using acidic ammonium molybdate with malachite green (16). The reaction mixtures (50 µl) contained 50 mM Tris-acetate pH 7.5, 50 mM sodium acetate, 0.1 mM EDTA, 10 mM $MgCl_2$, 0.1 mg/ml BSA, 1.5 µg ss M13mp18 DNA, NTP and enzyme. The reactions and phosphate determination were carried out as described previously (14).

Alternatively, ATP hydrolysis was monitored using a coupled assay (17). The reaction mixtures (1 ml) were as for the malachite green assay, but utilised $(dT)_{16}$ ssDNA. The reactions were initiated by the addition of PcrA and the rate of ATP hydrolysis was monitored by following NADH oxidation at 340 nm.

Analytical gel filtration

Gel filtration was performed at 22°C in the absence of nucleotide using a Superdex 200 HR 10/30 column. The column was equilibrated with 50 mM Tris pH 7.5, 2 mM EDTA, 2 mM DTT, 200 mM NaCl. The protein samples were concentrated using a Centricon 30 (Amicon). Protein sample (100 µl) was applied to the column. The apparent molecular weight (M_{app}) was calculated from an interpolation of a semi-log plot of partition co-efficient (K_{av}) of the protein markers versus molecular weights.

Chemical cross-linking of PcrA

PcrA, in the presence and absence of ligands, was treated with DMSI (18). A DMSI stock solution (50 mg/ml) was prepared in 0.5 M triethanolamine (TEA) pH 8.5 immediately prior to use. Cross-linking reactions were carried out in the following manner. PcrA (2 µM) in 50 mM TEA pH 8.5 + 40 mM NaCl, was mixed with the required ligands [combinations of 1.0 µM $(dT)_{16}$, 5 mM $MgCl_2$, 1 mM ADPNP, 1 mM ADP] and incubated at room temperature for 15 min. DMSI was added to a final concentration of 5 mg/ml and incubated at room temperature for 30 min. The reaction products were analysed using 7.5% SDS–PAGE.

SDS gel electrophoresis

Protein samples were analysed by SDS–PAGE in 7.5, 10, 12 and 15% gels with 4% stacking gels (19). Gels were stained with Coomassie Brilliant Blue and destained in 10% acetic acid and 25% methanol.

DNA mobility shift assays

The following oligonucleotides were used to make substrates for the binding reactions: 45mer (45o) and 22mer (22o) oligonucleotides as described by Crute *et al.* (15) and a 22mer (22c) oligonucleotide complementary to 22o, 5′-GCAGTGCTCGTTTT-3′ (LEB1), 5′-TTTTCGAGCACTGC-3′ (LEB2), 5′-GCAGTGCTCG-3′ (LEB3), 5′-CGAGCACTGC-3′ (LEB4). Fifty pmol of LEB1 and 22c were end-labelled by incubation with 50 µCi of [γ-^{32}P]ATP (3000 Ci/mmol) and 20 U T4 polynucleotide kinase for 90 min at 35°C followed by 10 min at 70°C. The unincorporated label was removed by centrifugation through a S-200 micro spin column (Pharmacia). Labelled oligonucleotide (5 pmol) was added to 45 pmol of unlabelled oligonucleotide and was either used as ssDNA substrate or was annealed to 50 pmol of complementary oligonucleotide. Binding reactions were carried out in 10 µl of 20 mM Tris pH 7.5, 120 mM NaCl, 3 mM $MgCl_2$, 5 mM DTT, 10% glycerol. Reaction mixtures were incubated at room temperature for 20 min and run at 10 V/cm on 4% polyacrylamide gels in 0.5× TBE. After electrophoresis the gel was dried under vacuum and auto-radiographed overnight at –80°C with Fuji RX X-ray film.

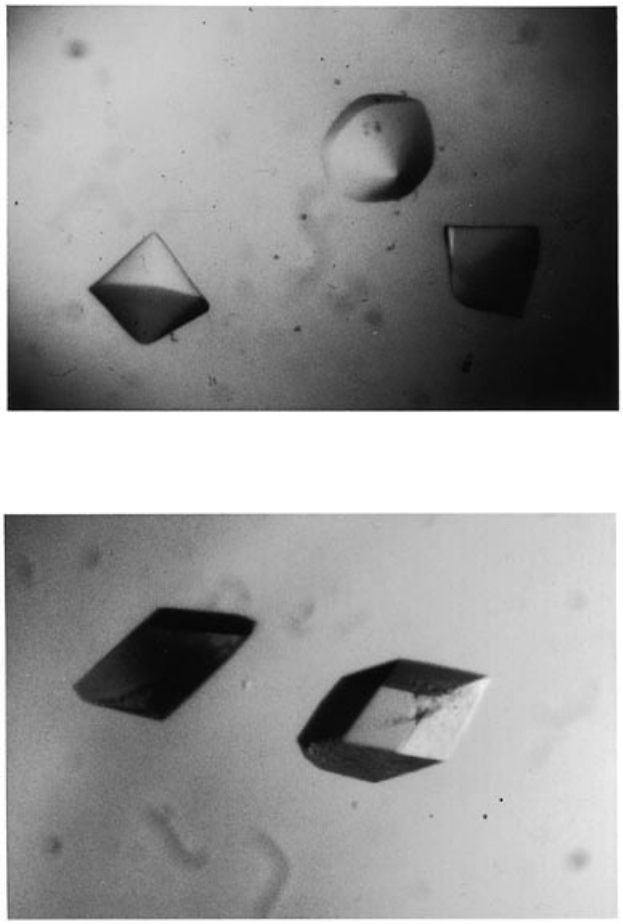

Figure 2. Crystals of PcrA. (**a**) Hexagonal bi-pyramids grown in the presence of 100 mM MES pH 6.4, 1.0 M sodium acetate. The largest crystals were 0.6 mm in their greatest dimension. (**b**) Parallelepiped crystals grown in the presence of 100 mM Tris pH 9.0, 2% (w/v) PEG8K, 3 mM ADP, 84 µM $(dT)_{10}$ and 10 mM $MgCl_2$. The largest crystals were 0.4 mm in their longest dimension.

RESULTS AND DISCUSSION

Crystallisation of PcrA

PcrA apo-crystals grew as hexagonal bipyramids which appeared overnight and grew to a maximum size of 0.4 × 0.4 × 0.6 mm over the course of a few days (Fig. 2a). The crystals were stable on exposure to X-rays and native data were collected to 2.5 Å resolution using synchrotron radiation and an image plate detector. The crystals belong to the space-group $P6_5$. The unit cell dimensions were a = b = 138.5 Å, c = 111.1 Å with one molecule per asymmetric unit and a solvent content of 65%. The model of PcrA built using these data has been described previously (11).

PcrA crystals grown in the presence of MgADP and ssDNA grew as parallelepipeds, appeared overnight, and grew to a maximum size of 0.4 × 0.15 × 0.15 mm (Fig. 2b). The crystals were also stable to X-rays and a 2.8 Å data set was collected. The crystals belong to the space group C2 with unit cell dimensions a = 130.2 Å, b = 90.1 Å, c = 82.6 Å, β = 116.7°, and contain one

molecule in the asymmetric unit. Preliminary analysis of the electron density map obtained by molecular replacement (data not shown) revealed that although ADP was bound, DNA was not. However, the structure obtained around the nucleotide binding site showed an identical conformation and contacts with ADP as those seen for the ADP soak in the original structural determination (11). In addition, the electron density for the C-terminal amino acids can be seen, a region that is disordered in the $P6_5$ crystals. The structure determination of this domain is underway.

Despite the high protein concentrations employed in the crystallisation of both crystal forms, the protein is monomeric with no obvious dimerisation interface. Furthermore, the crystallisation conditions (with regard to ionic strength, presence of ligands, etc.) were very different, suggesting that the monomeric state of the protein is likely to be representative of the protein in solution. The protein:protein contacts observed were typical of crystal contacts (i.e., involving just a few side chains) and were different in each case. Interestingly, since the determination of the PcrA structure, two other structures of helicases in Superfamilies I and II have been published, hepatitis C NS3 helicase and *E.coli* Rep helicase (20,21). The proteins were also monomeric in both of these structures.

Nucleotide specificity of PcrA

Many DNA helicases have broad nucleotide specificites. For example the bacteriophage T7 gene 4A and 4B proteins hydrolyse all naturally occurring nucleotides except CTP, with dTTP being the preferred substrate (22). *Escherichia coli* Rep hydrolyses ATP and dATP efficiently, with GTP and dGTP hydrolysed about one third less rapidly, while the remaining nucleotides are hydrolysed poorly (23). In contrast, UvrD hydrolyses only ATP and dATP efficiently (24). In order to examine the nucleotide specificity of PcrA, a DNA-dependent hydrolysis assay for a range of nucleotides was carried out using single-stranded M13 as an effector. NTP hydrolysis was monitored by analysing the production of inorganic phosphate using acidic ammonium molybdate with malachite green (16). In all cases Michaelis–Menten kinetics were observed. The kinetic parameters were determined by plotting velocity against velocity/[NTP] and are shown in Table 1. All the nucleotides utilised in this study were hydrolysed by PcrA. The kinetic parameters for all nucleotides were very similar, demonstrating that PcrA has a broad nucleotide substrate specificity. The kinetic parameters for the hydrolysis of ATP by PcrA in the absence of DNA were also determined. The k_{cat} for hydrolysis of ATP in the absence of DNA was 400-fold lower but K_m was decreased only by 5-fold. Thus the major affect of binding of ssDNA is on rate of turnover rather than K_m.

Since PcrA has a broad substrate specificity we investigated the ability of the enzyme to hydrolyse ethenoNTP analogues. The kinetic parameters for DNA-dependent hydrolysis of 3,N^4-ethenocytidine 5′-triphosphate (εCTP) and 1,N^6-ethenoadenosine 5′-triphosphate (εATP), using dT_{16} as an effector, were determined and are shown in Table 1. εCTP has two heterocyclic rings that are similar to the size of the rings in ATP but are arranged differently, while εATP has three heterocyclic rings. The enzyme is able to hydrolyse both analogues efficiently with similar values for k_{cat}. In fact, εATP is a better substrate for the NTPase activity than any of the naturally occurring NTPs tested.

Table 1. Steady-state kinetic parameters for the ATPase activity of PcrA

Nucleotide	K_m (mM)	k_{cat} (s^{-1})[a]
ATP	0.35	19
dATP	0.29	20
CTP	0.18	25
GTP	0.30	17
dGTP	0.25	19
dTTP	0.68	3
εATP	0.11	40
εCTP	0.29	42

[a]k_{cat} is expressed in terms of monomer.

The biochemical basis for the lack of specificity of PcrA can be seen in the structure of the binding site (11; Fig. 3). The binding site is very open and the principal interaction that ADP makes with the protein is through a stacking interaction of the adenine base with the side chain of Tyr286. The nature of this interaction explains why PcrA is able to bind and hydrolyse ethenonucleotides at least as well as other ribo- and deoxyribonucleotides.

PcrA can couple the hydrolysis of a range of nucleotides to helicase activity

The ability of a range of nucleotides to support the helicase reaction was also tested. PcrA can couple the hydrolysis of all the natural nucleotides tested to catalyse displacement of the oligonucleotide (Fig. 4). dTTP caused displacement of significantly less oligonucleotide, reflecting less efficient hydrolysis of dTTP compared with the other NTPs.

Helicase substrate specificity of PcrA

UvrD and Rep unwind duplex DNA with an attached 3′ ssDNA tail preferentially (25–27). In order to investigate the polarity of unwinding by PcrA, we used directionality substrates prepared from linearised M13mp18 and 22mer oligonucleotides (Fig. 5A) and looked at the efficiency of the enzyme to promote displacement of each of the oligonucleotides (Fig. 5B and C). There is a marked specificity for substrates with a 3′ tail, since the difference in concentration between the highest and lowest concentration is 20-fold and even at the highest concentration of protein all the oligonucleotide is not displaced for the 5′ tailed substrate. Thus, in common with Rep and UvrD, PcrA has a preference for 3′ tails. Although UvrD can unwind duplexes with a 5′ tail at high protein:DNA ratios, it has been shown that this was due to unwinding from the blunt end of duplexes (6). Rep can also unwind blunt duplexes but is less active than UvrD (6). In our assay system we cannot distinguish whether PcrA is unwinding at the blunt end or is utilising the 5′ tail of the substrate. The unwinding of the 5′ tailed substrate is incomplete even at a 5-fold excess of protein over DNA (nucleotides) suggesting that the activity of PcrA is more like that of Rep than of UvrD.

Dependence of ssDNA stimulated ATPase activity on length of DNA

The standard NTPase assay utilises bacteriophage M13 ssDNA as an effector of nucleotide hydrolysis. We have examined whether oligonucleotides can also stimulate the ATPase activity, since we wanted to define short oligonucleotides that were

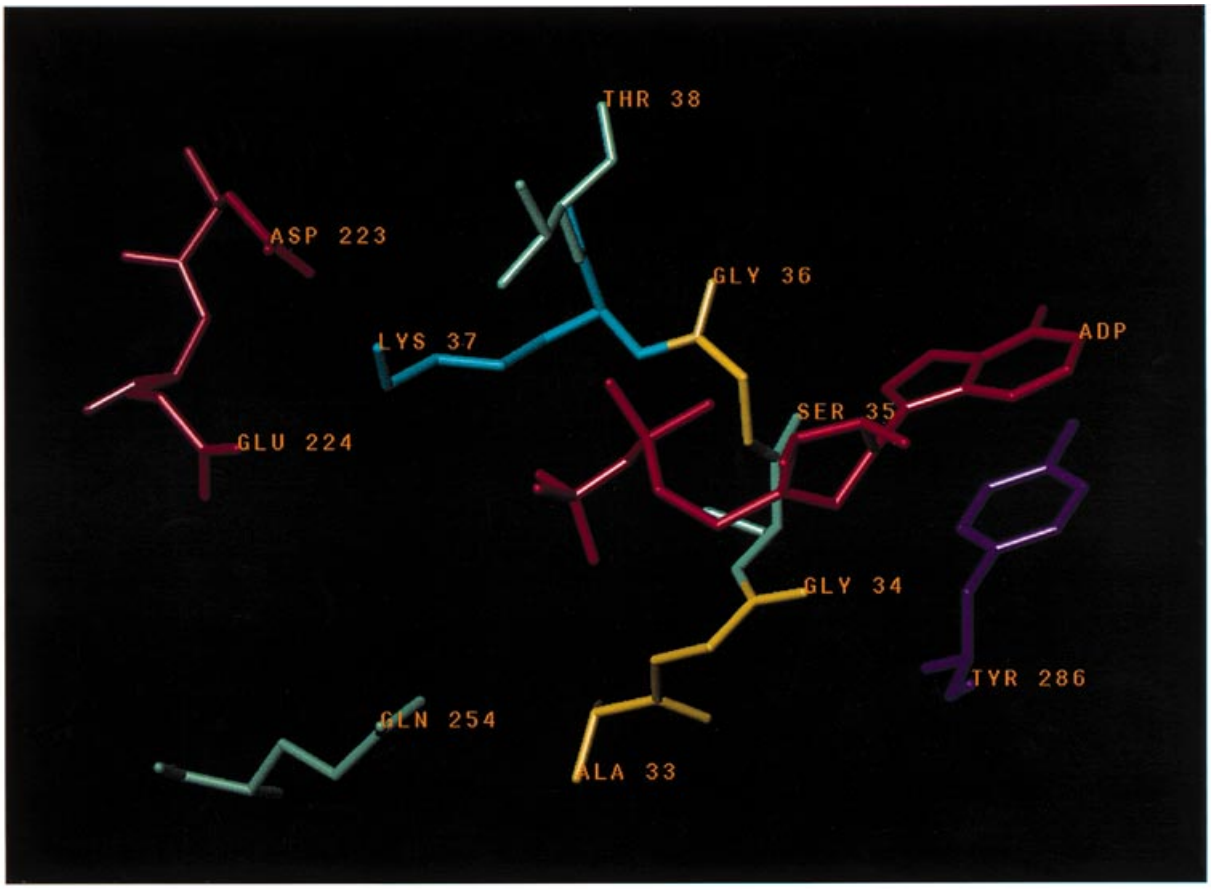

Figure 3. Structure of the nucleotide binding site of PcrA, showing residues that contact the ADP.

suitable for structural studies. The dependence of ATP hydrolysis on oligonucleotide concentration was measured using a coupled assay system. The concentration of DNA required for half-maximal stimulation of ATPase activity was determined and the results are shown in Table 2. In all cases the values for K_d are similar but decrease with increasing length. The values for k_{cat} were also very similar to each other and to that obtained with M13.

The results show that PcrA is able to use oligonucleotides as short as 4 bases to stimulate its NTPase activity but longer oligonucleotides do bind more tightly. From these data we cannot determine whether PcrA is binding to more than one molecule of DNA or if more than one molecule of PcrA is binding to one molecule of DNA. Indeed, in the Rep structure, two independent molecules are bound to a 16 base oligonucleotide, with each monomer covering 8 bases (21).

Table 2. K_d for differing lengths of oligo-dT

ssDNA	K_d (nM)
$(dT)_4$	590
$(dT)_{10}$	380
$(dT)_{12}$	250
$(dT)_{16}$	160

K_d was determined by analysing the dependence of the ATPase activity on DNA concentration at 3 mM ATP for a range of oligonucleotides. The data were analysed by plotting $1/(\Delta[NADH]s^{-1}$ against 1/[DNA].

DNA binding specificity of PcrA

The active rolling model of helicase action proposed by Wong and Lohman (28) necessitates the binding of helicase subunits alternately to ss and dsDNA. The alternating affinity is coupled to ATP binding and hydrolysis. However, it is unclear whether Rep is able to recognise the junction between ss and dsDNA. Interestingly, it appears that both PriA and RecG helicases bind preferentially to D-loops and branched structures with no observable binding to ss or dsDNA (29). We decided to examine the ability of PcrA to bind to ss (22c), 3′ ss tailed (45o + 22c) and dsDNA (22o + 22c; Fig. 6). The helicase binds equally effectively to ss and 3′ tailed DNA but less effectively to dsDNA. For binding of PcrA to the tailed substrate we cannot determine where the helicase is binding: it could be binding to the ds or the ss tail or at the junction between the ss and dsDNA. Examination of the electrostatic surface potential of PcrA using the program GRASP (30) showed that most of the protein is highly negative, with only the central cavity of the protein and a groove at the interface between subdomains 1A and 1B being positively charged (11). We therefore suggested that either or both of these regions could bind DNA (11). This proposal was confirmed by the structure of Rep complexed with ssDNA, in which the 5′ end of the DNA is bound across the central cavity formed by all four subdomains and the 3′ end is bound in the groove at the interface between subdomains 1A and 1B (21). In addition, in the PcrA structure there are basic residues that are on the front face of domain 1A

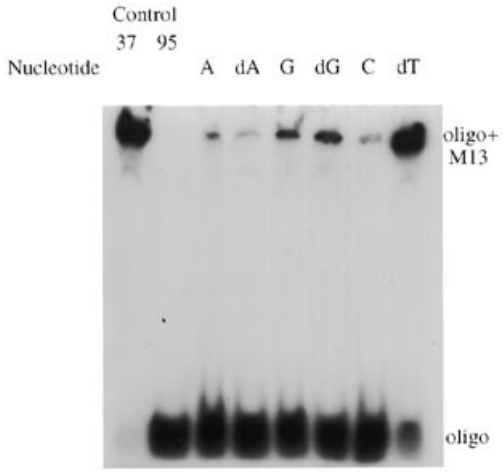

Figure 4. Dependence of the helicase activity of PcrA upon nucleotide. In all cases, the nucleotide concentration was 1 mM.

suggesting that this region of the protein may also bind DNA. Thus, a PcrA monomer could bind to a forked duplex structure. Since oligonucleotides as short as 4 bases stimulate the ATPase activity we designed and made a small, forked substrate by annealing the oligonucleotides LEB1 and LEB2, that has one turn of a DNA duplex and two 4 base tails. We also made the comparable substrate, by annealing LEB3 and LEB4 to make a 10 bp duplex. The ratio of protein:DNA required to shift the DNA suggests that PcrA binds the small substrate with tails better than the 22mer ssDNA (Fig. 7). Moreover, under comparable conditions, there is little or no binding to the 10 bp duplex that lacks the 4 base tails (data not shown). Thus, since PcrA binds the forked structure with higher affinity than the ss 22mer, it is unlikely that binding to the 4 base ssDNA alone could account for the increase in affinity for the forked structure. This suggests that, in common with PriA and RecG, PcrA shows DNA binding specificity for defined structures and that the presence of 4 base unpaired nucleotide tails is sufficient to stabilise binding to a 10 bp duplex. The specific binding of PcrA to this synthetic fork suggests this may be a closer analogue of the physiological substrate. This would be consistent with the suggestion by Jin *et al.* (31) that PcrA is loaded onto a forked substrate in the initiation of replication of plasmid pT181. It will be interesting to see what other structures are recognised by PcrA as this may give an insight into its role *in vivo*.

Dependence of the ATPase activity on the concentration of PcrA

It has been shown by Runyon *et al.* (32) that the ATPase activity of UvrD is dependent upon protein concentration. Below 1 nM monomer, k_{cat} is constant and then increases between 1 and 10 nM where a second plateau is reached. It was suggested that such behaviour is a result of dimerisation which stimulates the ATPase activity.

We have analysed k_{cat} between 0.1 and 200 nM PcrA and find no dependence on protein concentration. This could be due to a number of reasons, including that PcrA is already a dimer at 0.1 nM, that it does not dimerise in this concentration range, it is a monomeric protein or that there is no change in ATPase activity

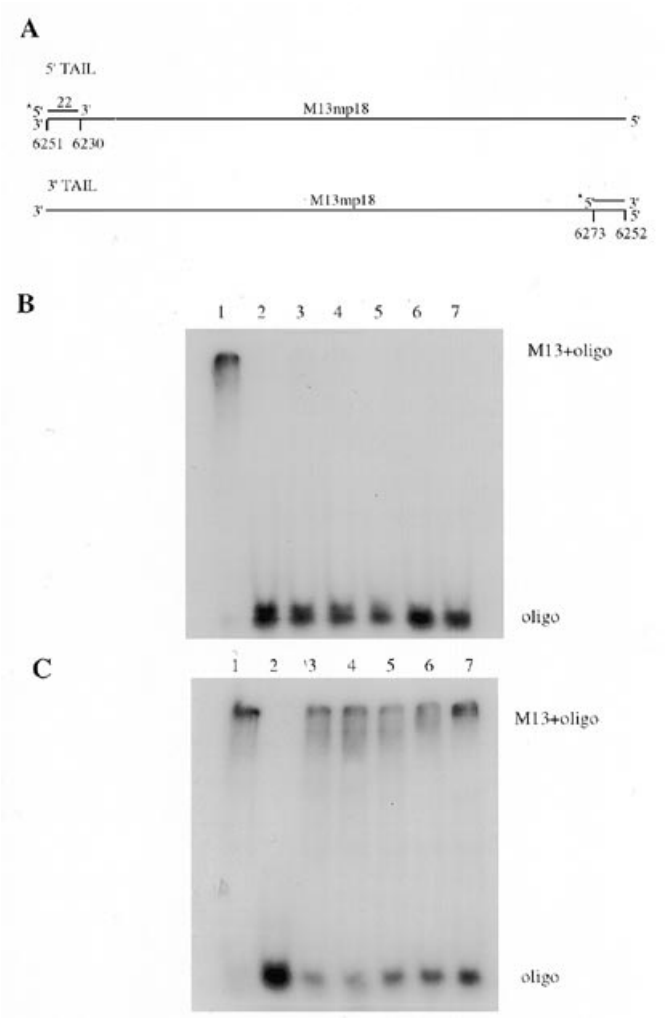

Figure 5. Substrate specificity of the helicase reaction. (**A**) 3′ and 5′ tailed substrates, (**B**) 3′ tailed substrate, (**C**) 5′ tailed substrate. In (B) and (C), reactions were carried out at 37°C, the DNA substrate concentration was 0.5 μM (in nucleotides) and 3 mM ATP was used as an energy source. Lanes 1, substrate alone at 37°C; lanes 2, substrate alone at 95°C; lanes 3, 0.125 μM PcrA; lanes 4, 0.25 μM PcrA; lanes 5, 0.5 μM PcrA; lanes 6, 1.0 μM PcrA; lanes 7, 2.5 μM PcrA.

on dimerisation. In order to distinguish between these possibilities we investigated the oligomeric state of PcrA.

Oligomerisation of PcrA

Rep helicase and UvrD are both reported to form dimers (32,33). UvrD in solution is in a monomer:dimer equilibrium, dimerisation being stimulated by ssDNA (32). In contrast, Rep is monomeric in solution and only forms dimers in the presence of ssDNA (33). We have used gel-filtration and chemical cross-linking to examine the oligomeric state of PcrA in the presence and absence of a variety of ligands.

In order to investigate the oligomeric state of PcrA in the absence of ligands, PcrA was applied to a Superdex 200 HR 10/30 column (Pharmacia) which had been calibrated using proteins of known molecular weight. A range of protein concentrations from 1 (12 μM) to 10 mg/ml (120 μM) was tested. In all cases, the protein eluted from the column with an apparent molecular weight

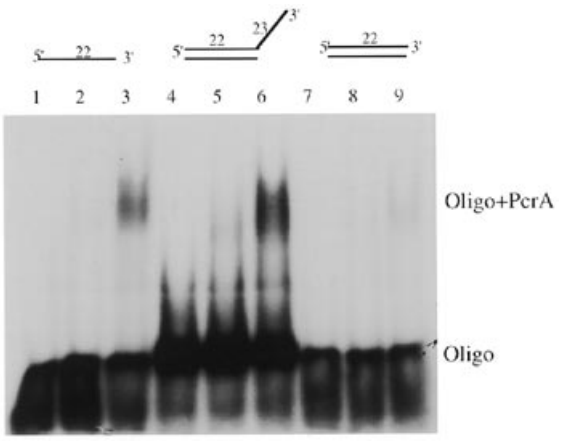

Figure 6. DNA binding specificity of PcrA. The oligonucleotide used in each group of lanes is shown above, and in all cases the concentration was 0.2 μM. Lanes 1–3, 22mer ssDNA; lanes 4–6, 3′ tailed duplex; lanes 7–9, 22mer duplex. The concentration of PcrA was 0, 0.7 and 2 μM, respectively, in each set of three lanes.

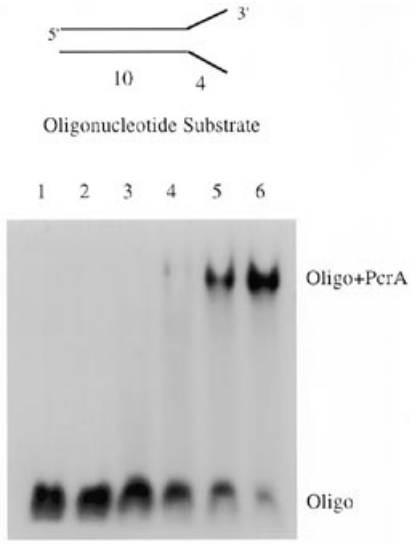

Figure 7. Band shift analysis of forked substrate. The structure of the forked substrate is indicated on the diagram. The duplex is 10 bp and the single stranded tails are $(dT)_4$. The oligonucleotide concentration was 0.5 μM. Lane 1, no PcrA; lane 2, 0.25 μM PcrA; lane 3, 0.5 μM PcrA; lane 4, 1.0 μM PcrA; lane 5, 2.0 μM PcrA; lane 6, 4.0 μM PcrA.

of 81 kDa, close to the predicted molecular weight of 82 kDa. This is in contrast to UvrD for which, even at considerably lower concentrations, the apparent molecular weight increases with increasing protein concentration until it reaches a plateau at the molecular weight equivalent to a dimer, indicating a monomer/dimer equilibrium in rapid exchange (32). Since the dimerisation of both Rep and UvrD are stimulated by binding to ssDNA (32,33), the oligomeric state of PcrA in the presence of ligands was examined by chemical cross-linking (Fig. 8). In all cases a small amount of higher order oligomers was observed as well as an internal cross-link which is diminished in the presence of DNA. However, binding of DNA does not increase the amounts

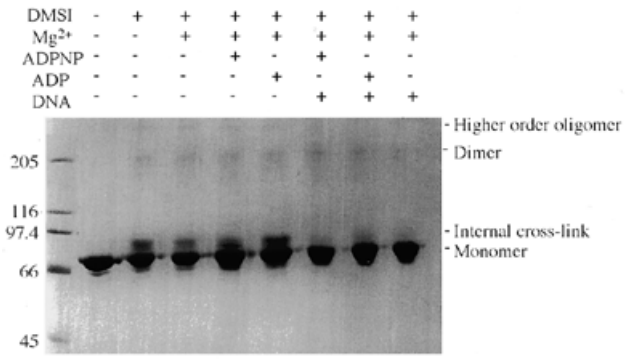

Figure 8. Chemical cross-linking of PcrA with DMSI. The reaction conditions were as described in Materials and Methods. The additives to the protein are indicated above each lane. Lane 1 contains molecular weight markers. The positions of monomer, internally cross-linked monomer and other oligomers are indicated.

of higher order oligomers that are observed. Since gel filtration of PcrA in the absence of ligands shows only monomeric protein, and the degree of cross-linking is unaltered by the presence of ligands, it is most likely that the small amount of cross-linking that is observed is non-specific. The linearity of the dependence of the ATPase activity upon protein concentration also points to the protein being monomeric under these conditions, since both Rep and UvrD show a stimulation of rate as the protein dimerises. Thus, under a wide range of experimental conditions we fail to demonstrate any significant dimerisation of PcrA.

The lack of observable dimerisation for PcrA is inconsistent with the active rolling model of helicase action (28). This model has two fundamental requirements: (i) the enzyme must have an oligomeric structure in which pairs of subunits act cooperatively, and (ii) each subunit binds either ss or dsDNA at any instant, but not simultaneously. This model has been popularised by its proponents and a large amount of kinetic and biochemical data have been published in its support (reviewed in ref. 1). However, there is a growing body of evidence that is difficult to reconcile with this model. Despite considerable efforts, we have failed to demonstrate any dimerisation of PcrA. As discussed previously, all three published structures are of monomeric proteins even when DNA is bound. The structure of Rep bound to ssDNA revealed two monomers of Rep bound to the 16 base oligonucleotide (21). The observation of monomeric Rep in the crystal was particularly surprising since the oligonucleotide used was the same as that used to demonstrate dimerisation of Rep (33), yet the structure shows clearly how two Rep monomers could be accomodated adjacent to each other on a single DNA molecule, with each monomer covering 8 bases of ssDNA. Moreover, the step size of 4–5 bp demonstrated recently for the closely related helicase, UvrD (34) also appears incompatible with the rolling model, since this step size is considerably smaller than the region of DNA covered by the Rep monomer. If one assumes that hexameric helicases operate via a similar mechanism it is unclear how they might roll, since the DNA passes through the centre of the ring (35,36), again questioning whether the rolling model can be a general mechanism for helicases. With regard to the binding of helicases to either ds or ssDNA, our data suggest not only that PcrA can bind both ss and dsDNA simultaneously but that the enzyme actually has a higher affinity for these substrates (i.e., forks)

than for either ds or ssDNA, an observation that is also at odds with the rolling model.

An alternative mechanism is the inchworm model (26), in which the enzyme travels along the dsDNA unwinding the duplex as it goes. Although in the original model it was proposed that two ATPs were hydrolysed per base pair unwound, and therefore that the step size for each cycle was one, this was based on an assumption about the efficiency of coupling of the helicase to ATPase activities that is likely to be an overestimate. Consequently, a small variation of this model could accomodate a number of base pairs being unwound for each ATP hydrolysed and could thus be compatible with the step size of 4–5 bp observed for UvrD. Perhaps the most important difference between the two models is that, in the inchworm model, the enzyme need not be oligomeric. The multifunctional enzyme complex RecBCD has a 3′–5′ helicase activity amongst its functions, and a monomeric heterotrimer has been shown to be the active unit (37). It is the RecB protein that confers the helicase activity upon the complex (38), while the other components of the complex stimulate this activity (39). The active complex therefore contains a single helicase molecule. Consequently, it has been suggested that these observations of the oligomeric state of the active complex are inconsistent with the rolling model (37,39). Moreover, the oligomeric state in both crystal forms of PcrA, as well as those of NS3 helicase and Rep, the lack of observable dimerisation or cooperativity in ATPase kinetics for PcrA, and the step size of 4–5 bp unwound per cycle for UvrD are all consistent with an inchworm model. It may be that the dimerisation and kinetics of ATP hydrolysis for Rep and UvrD are of biological rather than mechanistic importance. We therefore believe it to be premature to discredit alternatives to the rolling model and we must await further structural and kinetic data to resolve the mechanism of helicase action.

ACKNOWLEDGEMENT

This work was supported by the Wellcome Trust.

REFERENCES

1 Lohman,T.M. and Bjornson,K.P. (1996) *Annu. Rev. Biochem.*, **65**, 169–214.
2 Matson,S.W. and Kaiser-Rogers,K.A. (1990) *Annu. Rev. Biochem.*, **59**, 289–329.
3 Schmid,S.R. and Linder,P. (1992) *Mol. Microbiol.*, **6**, 283–292.
4 Gorbalenya,A.E. and Koonin,E.V. (1993) *Curr. Opin. Struct. Biol.*, **3**, 419–429.
5 LeBowitz,J.H. and McMacken,R., (1986) *J. Biol. Chem.*, **261**, 4738–4748.
6 Matson,S.W., Tabor,S. and Richardson,C.C. (1983) *J. Biol. Chem.*, **258**, 14017–14024.
7 Runyon,G.T. and Lohman,T.M. (1989) *J. Biol. Chem.*, **264**, 17502–17512.
8 Iordanescu,S. (1993) *Mol. Gen. Genet.*, **241**, 185–192.
9 Denhardt,DT. (1975) *CRC Crit. Rev. Microbiol.*, **4**, 161–223.
10 Eisenberg,S., Scott,J.F and Kornberg,A. (1976) *Proc. Natl. Acad. Sci. USA*, **73**, 3151–3155.
11 Subramanya,H.S., Bird,L.E., Brannigan,J.A. and Wigley,D.B. (1996) *Nature*, **384**, 379–383.
12 Sambrook,J., Fritsch,E.F. and Maniatis,T. (1989) *Molecular Cloning: A Laboratory Manual*. 2nd Edition. Cold Spring Harbour Laboratory Press, Cold Spring Harbor, NY.
13 Otwinowski,Z. (1993) In Sawyer,L., Isaacs,N. and Bailey,S. (eds), *Data Collection and Processing*. SERC Laboratory, Daresbury, UK, pp. 56–62.
14 Bird,L.E., Håkansson,K., Pan,H. and Wigley,D.B. (1997) *Nucleic Acids Res.*, **25**, 2620–2626.
15 Crute,J.J., Mocarski,E.S. and Lehman,I.R. (1988) *Nucleic Acids Res.*, **16**, 6585–6596.
16 Lanzetta,P.A., Alvarez,L.J., Reinach,P.S. and Candia,O.A. (1979) *Anal. Biochem.*, **100**, 95–97.
17 Pullman,M.E., Penefsky,A., Datta,A. and Racker,E. (1960) *J. Biol. Chem.*, **235**, 3322–3329.
18 Davies,G.E. and Stark,G.R. (1970) *Proc. Natl. Acad. Sci. USA*, **66**, 651–656.
19 Laemilli,U.K. (1970) *Nature*, **227**, 680–685.
20 Yao,N., Hesson,P., Cable,M., Hong,Z., Kwong,A.D., Le,H.V. and Weber,P.C. (1997) *Nature Struct. Biol.*, **4**, 463–467.
21 Korolev,S., Hsieh,J., Gauss,G.H., Lohman,T.M. and Waksman,G. (1997) *Cell*, **90**, 635–647.
22 Matson,S.W. and Richardson,C.C. (1983) *J. Biol. Chem.*, **258**, 14009–14016.
23 Kornberg,A., Scott,J.F. and Bertsch,L.L. (1978) *J. Biol. Chem.*, **253**, 3298–3304.
24 Matson,S.W. and George,J.W. (1987) *J. Biol. Chem.*, **262**, 2066–2076.
25 Matson,S.W. (1986) *J. Biol. Chem.*, **261**, 10169–10175.
26 Yarranton,G.T. and Geftner,M.L. (1979) *Proc. Natl. Acad. Sci. USA*, **76**, 1658–1662.
27 Lohman,T.M., Chao,K., Green,J.M., Sage,S. and Runyon,G.T. (1989) *J. Biol.Chem.*, **264**, 10139–10147.
28 Wong,I. and Lohman,T.M. (1992) *Science*, **256**, 350–355.
29 McGlynn,P., Al-Deib,A.A., Liu,J., Marians,K.J. and Lloyd,R.G. (1997) *J. Mol. Biol.*, **270**, 212–221.
30 Nicholls,A. and Honig,B. (1991) *J. Comput. Chem.*, **12**, 435–445.
31 Jin,R., Fernandez-Beros,M.-E. and Novick,R.P. (1997) *EMBO J.*, **16**, 4456–4466.
32 Runyon,G.T., Wong,I. and Lohman,T.M. (1993) *Biochemistry*, **32**, 602–612.
33 Chao,K. and Lohman,T.M. (1991) *J. Mol. Biol.*, **221**, 1165–1181.
34 Ali,J.A. and Lohman,T.M. (1997) *Science*, **275**, 377–380.
35 Stasiak,A., Tsaneva,I.R., West,S.C., Benson,C.J.B., Yu,X. and Egelman,E.H. (1994) *Proc. Natl. Acad. Sci. USA*, **91**, 7618–7622.
36 Egelman,E.H., Yu,X., Wild,R., Hingorani,M. and Patel,S.S. (1995) *Proc. Natl. Acad. Sci. USA*, **92**, 3869–3873.
37 Taylor,A.F. and Smith,G.R. (1995) *J. Biol. Chem.*, **270**, 24451–24458.
38 Boehmer,P.E. and Emmerson,P.T. (1992) *J. Biol.Chem.*, **267**, 4981–4987.
39 Phillips,R.J., Hickleton,D.C., Boehmer,P.E. and Emmerson,P.T. (1997) *Mol. Gen. Genet.*, **254**, 319–329.